



ORIGINAL ARTICLE

# Investigation of intercalation of diphenhydramine into the interlayer of smectite by XRD, FTIR, TG-DTG analyses and molecular simulation



Guocheng Lv <sup>a,\*</sup>, Po-Hsiang Chang <sup>b</sup>, Xuebing Xing <sup>a</sup>, Wei-Teh Jiang <sup>b</sup>, Jiin-Shuh Jean <sup>b</sup>, Zhaohui Li <sup>a,b,c,\*</sup>

<sup>a</sup> Beijing Key Laboratory of Materials Utilization of Nonmetallic Minerals and Solid Wastes, National Laboratory of Mineral Materials, School of Materials Science and Technology, China University of Geosciences, Beijing, 29 Xueyuan Road, Beijing 100083, China

<sup>b</sup> Department of Earth Sciences, National Cheng Kung University, 1 University Road, Tainan 70101, Taiwan

<sup>c</sup> Geosciences Department, University of Wisconsin – Parkside, Kenosha, WI 53141-2000, USA

Received 22 December 2014; accepted 18 April 2015

Available online 25 April 2015

## KEYWORDS

Dehydration;  
Diphenhydramine;  
Intercalation;  
Molecular dynamic simulation;  
Smectite

**Abstract** Diphenhydramine (DPH) is one of the pharmaceuticals commonly found in the effluent stream after wastewater treatment, and the cause of its environmental persistence needs to be addressed urgently. Smectite minerals are common soil components with large surface area, expandable interlayer, and high cation exchange capacity (CEC), thus are capable of adsorbing or intercalating inorganic or organic cations on the surface or in the interlayer. In this study the intercalation of DPH in the interlayer of a Ca-smectite was characterized by X-ray diffraction, infra-red, and thermogravimetric analyses supported by molecular dynamic simulation. At the low (0.2–0.3 CEC) and high (0.6–0.7 CEC) adsorption levels, the intercalated DPH might take a horizontal monolayer or a bilayer configuration, resulting in a  $d_{001}$  expansion to 15 or 17 Å, respectively. As the amount of DPH intercalation increased, a gradual, yet systematic, dehydration due to removal of hydrated inorganic cation  $\text{Ca}^{2+}$  from the interlayer was observed. In addition, the intercalated DPH had a slightly higher thermal stability due to the shield effect of the host mineral smectite against heat. The uptake of DPH by the smectite was attributed to both electrostatic interactions between the negatively charged mineral surfaces and the positively charged tertiary

\* Corresponding authors at: Geosciences Department, University of Wisconsin – Parkside, Kenosha, WI 53141-2000, USA. Tel.: +1 262 595 2487 (Z. Li).

E-mail addresses: [Guochenglv@cugb.edu.cn](mailto:Guochenglv@cugb.edu.cn) (G. Lv), [li@uwp.edu](mailto:li@uwp.edu) (Z. Li).

Peer review under responsibility of King Saud University.



amine and cation exchange interactions between DPH<sup>+</sup> and hydrated Ca<sup>2+</sup>. Thus, smectite minerals could serve as a sink to remove dissolved DPH from water on the one hand, and as a carrier to transport intercalated DPH in the environment on the other hand.

© 2015 The Authors. Production and hosting by Elsevier B.V. on behalf of King Saud University. This is an open access article under the CC BY-NC-ND license (<http://creativecommons.org/licenses/by-nc-nd/4.0/>).

## 1. Introduction

Extensive use of pharmaceutical in modern society resulted in their frequent detection in both natural streams and the effluent after wastewater treatment. These pharmaceuticals include antibiotics and other commonly used over-the-counter medicines. Diphenhydramine (DPH) is a widely used over-the-counter antihistamine. It is the active ingredient of Benadryl used to alleviate the symptoms associated with allergy. The primary mechanism of action for DPH is antagonism of the histamine H<sub>1</sub> receptor, which blocks histamine from binding to receptors and reduces histamine-mediated allergic responses (Goolsby et al., 2013). As it is an over-the-counter medicine, it was one of the mostly overused drugs. In 2003, there were 28,092 human exposures to DPH reported to poison centers in the US, among which 11,355 (40.4%) were evaluated in a healthcare facility and children less than 6 years of age accounted for 12,089 (43.0%) (Scharman et al., 2006).

DHP along with azithromycin, caffeine, 1,7-dimethylzanthine, carbamazepine, cotinine, DEET, and sulfamethazine was detected at all locations at four rivers downstream of wastewater treatment plants (WWTPs) with trickling filters or trickling filters in parallel with activated sludge streams plus a discharge canal at Nebraska, USA and WWTP effluent was attributed to be a significant source of pharmaceutical loading to the receiving waters (Bartelt-Hunt et al., 2009). Up to 70 ng/L was detected in tributaries of the Columbia River Basin (Nilsen et al., 2014) and up to 1.8 µg/L was detected in the influent of wastewater (Li et al., 2013). Concentrations up to lower micrograms per liter levels in effluent and in surface waters downstream from WWTP discharges were also reported (Bartelt-Hunt et al., 2009). DPH is not eliminated efficiently during wastewater treatment and considerable amounts are sequestered into biosolids (Wu et al., 2010a). Biosolids from the WWTPs could accumulate up to 22 mg/kg with a median concentration of 340 µg/kg of DPH (Kinney et al., 2006).

In addition to its frequent detection in surface water and wastewater, DPH is extremely persistent in agricultural soil (Topp et al., 2012). Over the 110 day experimental period, DPH showed no dissipation after biosolids applied to soils with and without plants (Wu et al., 2010b). And the time to dissipate 50% of DPH may take up to a year in loam soil (Topp et al., 2012).

DPH is very stable under UV under non-catalytic conditions but complete degradation and considerable mineralization (ca. 60–70%) under near UV to visible irradiation (50 mW cm<sup>-2</sup>) could be achieved in 60 min by selecting the appropriate TiO<sub>2</sub> loading (Pastrana-Martínez et al., 2012). No discernable loss of DPH was found over 3 years of monitoring of an outdoor mesocosm study in Baltimore, Maryland (Walters et al., 2010).

The adsorption of DPH in environmental matrixes was rarely reported, although a limited mobility was observed due to its high sorption on soils (Wu et al., 2010a). A large distribution coefficient (log *K*<sub>OW</sub> of 3.27) indicated its strong affinity for soils (Kinney et al., 2006). On the other hand, studies of DPH adsorption on activated carbon (AC) were assessed *in vitro* and *in vivo* in six healthy volunteers in order to evaluate the utility of AC as an adjunct in the treatment of antihistamine overdose (Guay et al., 1984). Their results showed that at an AC to DPH ratio of 10:1, 85% of the DPH was adsorbed. Maximum DPH adsorption on dehydrated and activated carbon prepared from date palm took place at pH 8.0 (El-Shafey et al., 2014). Addition of strongly cationic exchange resin resulted in significant decrease in DPH release (Akkaramongkolporn et al., 2010).

Given the facts of extensive detection of DPH in the environment and limited studies on interactions between DPH and environmental matrix, we studied the removal of DPH by swelling clay minerals (Li et al., 2011a), in which extensive uptake of DPH by the clay minerals was observed and cation exchange reaction was attributed to the DPH uptake. In this study, we extended our research to detailed material characterization after adsorbing different amounts of DPH under different physicochemical conditions in order to further elucidate the states of the presence of adsorbed DPH in the interlayer of smectite. In addition, the protection of DPH intercalated in the smectite interlayer from thermal decomposition was discussed in detail.

## 2. Materials and methods

The smectite used was a high-charge Ca-montmorillonite (SAz-1) obtained from the Clay Mineral Repositories in Purdue University (West Lafayette, IN) with a cation exchange capacity (CEC) of 123 ± 3 meq/100 g (Borden and Giese, 2001), an external surface area of 65 m<sup>2</sup>/g (Dogan et al., 2006), and a layer charge of 0.35 eq/mol per (Si,Al)<sub>4</sub>O<sub>10</sub> (Mermut and Lagaly, 2001). As it contains more than 98% of montmorillonite (Chipera and Bish, 2001), it was used as is without further purification.

The diphenhydramine HCl (CAS #: 147-24-0) was provided by Wei Li Pharmaceutical Co. Ltd. (Tainan, Taiwan). It is a weak base with a p*K*<sub>a</sub> value of 9.0 (Mizuuchi et al., 1999), corresponding to the protonation of the tertiary amine in the molecule (Fig. 1). It has a molecular weight of 291.82 g/mol a water solubility of 3 g/L and a log *K*<sub>OW</sub> value of 3.27 (Kinney et al., 2006).

The smectite was equilibrated with DPH for 24 h at the following initial concentrations: 0, 50, 100, 200, 400, 600, 800, 1000, 1500, and 2000 mg/L, or at an initial concentration of 1000 mg/L for the following time: 1, 2, 5, 10, 15, 30, 60, 120, 240, 480, and 1440 min, or at an initial concentration of

1000 mg/L for 24 h under equilibrium pH 2–11. The mixtures were shaken at 150 rpm for varying amounts of time or 24 h, centrifuged at 7600 rpm for 20 min, and the supernatants were filtered through 0.45  $\mu\text{m}$  syringe filters before the equilibrium DPH concentrations were measured by a UV–Vis spectrophotometer method (SmartSpec 3000, Bio-Rad Corp.) at the wavelength of 254 nm (Tipparat et al., 2002).

The powder XRD analyses were performed on a Rigaku D/max-IIIa diffractometer with a Ni-filtered  $\text{CuK}\alpha$  radiation at 30 kV and 20 mA and the samples were scanned from  $2^\circ$  to  $10^\circ 2\theta$  at  $1^\circ/\text{min}$  with a scanning step of  $0.01^\circ/\text{step}$ , as the

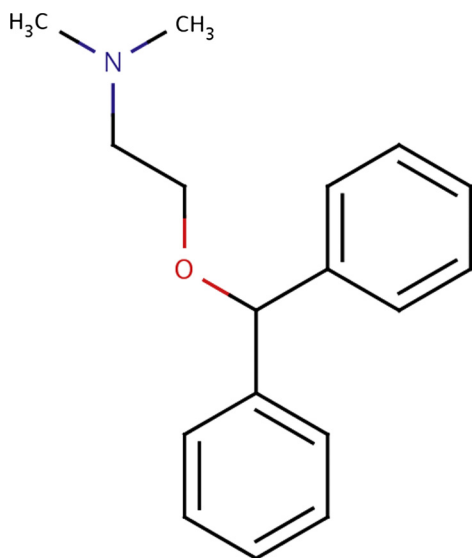


**Figure 1** Diphenhydramine molecular structure.

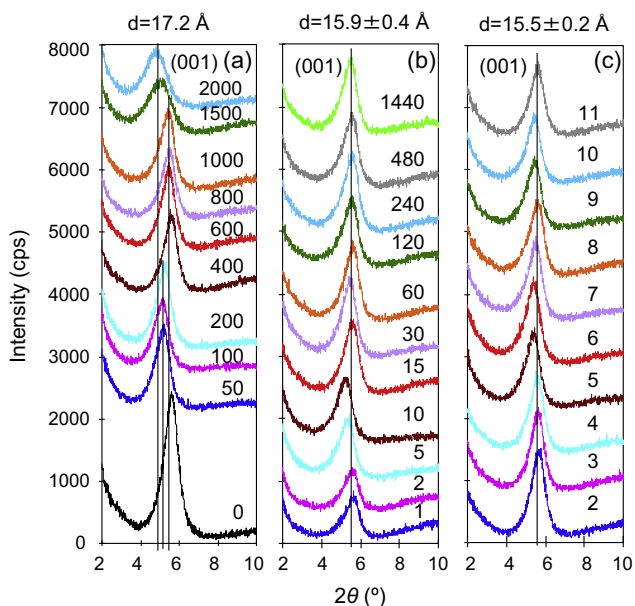


**Figure 2** X-ray diffraction patterns of SAz-1 after in contact with different initial concentrations (mg/L) of DPH (a); at different contact time (min) with an initial concentration of 1000 mg/L (b); and under different equilibrium pH values with an initial concentration of 1000 mg/L (c).

DPH-adsorbed samples did not exhibit separate DPH peaks beyond  $10^\circ$ .

The TG-DTG analyses were performed on a Pyris Diamond TG/DTA (Perkin Elmer). The heating rate was  $10^\circ\text{C}/\text{min}$  under air. The initial sample weight was between 6 and 15 mg.

The FTIR spectra were acquired on a Bruker Equinox 55 Spectrometer using KBr pressing method. The spectra were

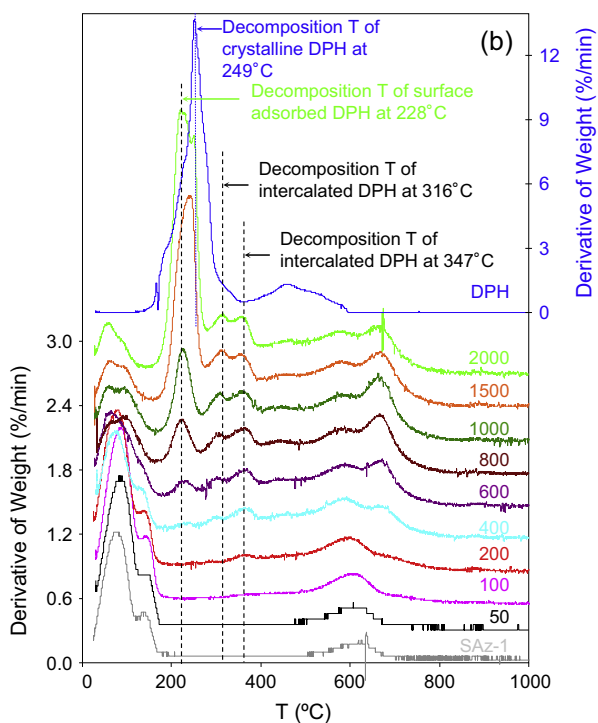
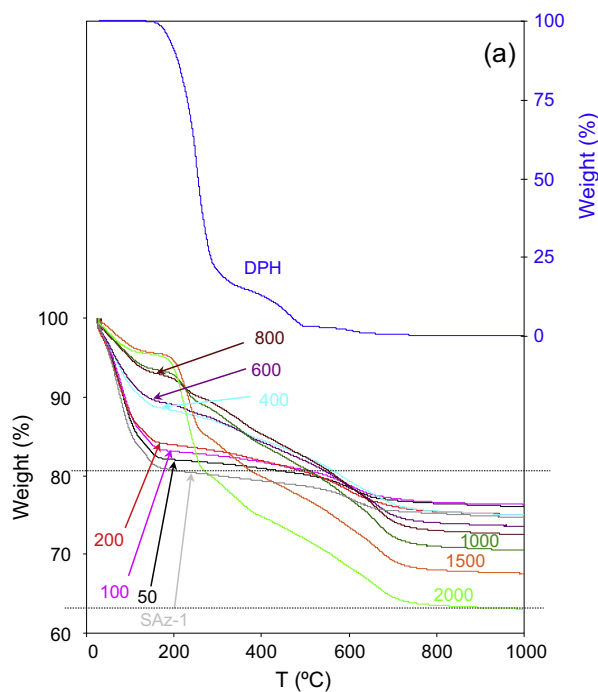


**Figure 3** TG (a) and DTG (b) analyses of SAz-1 after in contact with different initial concentrations (mg/L) of DPH. The right y-axis is for DPH.

collected by accumulating 256 scans at a resolution  $4 \text{ cm}^{-1}$  from 600 to  $4000 \text{ cm}^{-1}$ .

Molecular dynamic (MD) simulation was performed using the module Forcite of Materials Studio 5.0 software to investigate configuration of intercalated DPH molecules under different loading levels in smectite. The supercell of the model was made of 8 smectite unit cells at  $4a \times 2b \times 1c$ . The chemical formula of the smectite used was  $(\text{Ca}_{0.55}\text{K}_{0.01})[\text{Al}_{2.67}\text{Fe}_{0.15}\text{Mg}_{1.20}][\text{Si}_{8.00}]\text{O}_{20}(\text{OH})_4$  (Breen et al., 1995). It was assumed that the layer charge came from the substitution of aluminum by magnesium in the octahedral sheets and the total layer charge was  $-8$  balanced by  $4 \text{ Ca}^{2+}$  in the interlayer. A dimension of  $11 \text{ \AA} \times 9.6 \text{ \AA} \times 4.0 \text{ \AA}$  was assumed to be the molecular size of DPH (Li et al., 2011a). The DPH adsorption capacity was  $0.88 \text{ mmol/g}$ , determined by a batch adsorption study (Li et al., 2011a). At this DPH adsorption level, 6 of the 8 charges from  $\text{Ca}^{2+}$  ions would be substituted by  $\text{DPH}^+$ .

The established model was optimized geometrically. The temperature was set at  $298 \text{ K}$  and time was at  $1 \text{ ns}$  with a time step of  $1 \text{ fs}$ . Universal force field was used during simulation. The Ewald summation method was used to calculate the electrostatic interaction. After the system reached equilibrium, the NVT kinetic simulation was performed under the same time constant and temperature conditions. The data were collected on the last  $500 \text{ ps}$  for later analyses.

### 3. Results and discussion

#### 3.1. XRD of DPH-adsorbed smectite

The XRD pattern of crystalline DPH matched with that previously published well and the strongest peak at  $12.3^\circ 2\theta$  confirmed the HCl form of DPH (Nandgude et al., 2008). The d-spacing of the raw SAz-1 was  $15.0 \text{ \AA}$ , confirming that  $\text{Ca}^{2+}$  was the interlayer cation with two layers of interlayer water (Fig. 2). Adsorption of different amounts of DPH resulted in a systematic increase in d-spacing from  $15.0$  to  $17.2 \text{ \AA}$  as the initial DPH concentrations increased. This increase suggested certain portions of the adsorbed DPH molecules were retained in the interlayer space of SAz-1, resulting in intercalation. The XRD patterns of SAz-1 in contact with  $1000 \text{ mg/L}$  under different equilibrium time did not show much difference. The mean d-spacing was  $15.9 \pm 0.4 \text{ \AA}$

(Fig. 2b). The invariable d-spacing may suggest that the adsorption of DPH on SAz-1 was instantaneous, similar to a previous observation (Li et al., 2011a). Similarly, a d-spacing of  $15.5 \pm 0.2 \text{ \AA}$  was found for SAz-1 after in contact with  $1000 \text{ mg/L}$  DPH for  $24 \text{ h}$  under different equilibrium pH conditions (Fig. 2c). This latter case may suggest that the interlayer configuration of DPH in SAz-1 is not sensitive to pH changes.

In addition to changes in d-spacing after intercalation of different amounts of DPH, a moderate increase in full width at half height of the  $(001)$  peak was noticed for smectite after in contact with DPH in comparison with raw smectite, particularly for the samples at initial concentrations of  $1500$  and  $2000 \text{ mg/L}$  (Fig. 2a). This increase reflects a slight decrease in crystalline size, particularly the number of stacking layers along  $c$  direction.

#### 3.2. TG-DTG analyses

The endothermic peak at  $171^\circ \text{C}$  and exothermic peak at  $232^\circ \text{C}$  of crystalline DPH corresponded to the melting and decomposition points, respectively (Agresti et al., 2008; Nandgude et al., 2008). In a separate study,  $92\%$  of weight loss of DPH was found in one degradation step at  $190\text{--}330^\circ \text{C}$  (Ulu and Elmali, 2010). In this study, the peak decomposition temperature of crystalline DPH was at  $249^\circ \text{C}$  with a shoulder at  $182^\circ \text{C}$  (Fig. 3b). Since the heating rate was the same ( $10^\circ/\text{min}$ ), the difference in results obtained from this study and from Nandgude et al. (2008) could be originated from the difference in ambient gas condition as air was used in this study while nitrogen purge was used in Nandgude et al. (2008) study. It may also indicate that melting and decomposition occurred simultaneously in air. A derivative of thermogravimetric (DTG) maximum of  $244^\circ \text{C}$  was found with a heating rate of  $10^\circ/\text{min}$  in an inert argon atmosphere (Zayed and El-Habeeb, 2010).

For raw smectite, the weight loss was about  $19\%$  at  $180^\circ \text{C}$  (Fig. 3a and Table 1), in agreement with the weight loss conducted without  $\text{N}_2$  purge (Guggenheim and Van Groos, 2001). This weight loss corresponded to the removal of adsorbed plus interlayer water. As the amount of DPH adsorbed increased continuously from  $0.07$ ,  $0.13$ , to  $0.27 \text{ mmol/g}$ , the weight loss at this temperature range decreased systematically from  $19\%$

**Table 1** Weight loss at  $200$  and  $800^\circ \text{C}$  and derivative of weight loss at different peak temperatures.

Samples	Amount of DPH uptake (mmol/g)	TG weight loss at $180^\circ \text{C}$ (%)	TG weight loss at $800^\circ \text{C}$ (%)	DTG peak at $77^\circ \text{C}$ (%/min)	DTG peak at $144^\circ \text{C}$ (%/min)	DTG peak at $228^\circ \text{C}$ (%/min)	DTG peak at $316^\circ \text{C}$ (%/min)	DTG peak at $347^\circ \text{C}$ (%/min)
DPH	–	–	100	0.0	0.0	Shoulder	0.0	0.0
Raw smectite	–	19	26	1.2	0.1	0.0	0.0	0.0
50 mg/L	.03	18	23	1.2	0.1	0.0	0.0	0.0
100 mg/L	.07	16	23	1.1	0.1	0.0	0.0	0.0
200 mg/L	.13	15	24	1.1	0.1	0.0	0.0	0.05
400 mg/L	.27	12	25	0.9	0.05	0.1	0.1	0.1
600 mg/L	.39	11	26	0.7	0.0	0.2	0.1	0.15
800 mg/L	.51	7	27	0.6	0.0	0.4	0.15	0.2
1000 mg/L	.63	7	29	0.5	0.0	0.6	0.15	0.2
1500 mg/L	.80	4	32	0.4	0.0	1.5	0.2	0.3
2000 mg/L	.88	4	37	0.3	0.0	1.8	0.2	0.3

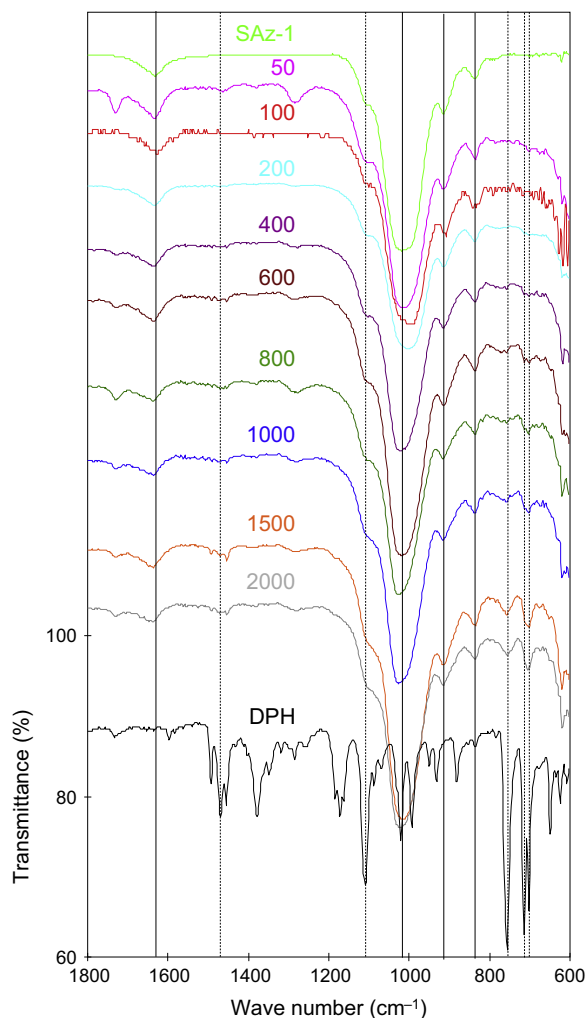


**Figure 4** FTIR analyses of SAz-1 in contact with DPH at different initial concentrations (mg/L) at 600–1800  $\text{cm}^{-1}$ .

to 15% (Fig. 3a). On the DTG graph, the major peak was due to removal of adsorbed and interlayer water. The DPH peak at 249 °C was absent at these low DPH adsorption levels (Fig. 3b). At the intermediate DPH adsorption level, the weight loss at 180 °C was further reduced to 10–11% (Fig. 3a), reflecting continuous dehydration of smectite as the amount of DPH adsorbed increased. Meanwhile, a DTG peak at 228 °C began to appear, which may be due to decomposition of the surface adsorbed DPH (Fig. 3b). At higher amount of DPH adsorption the weight loss at 180 °C was only 5% (Fig. 3a), and the DTG peak at 228 °C increased significantly (Fig. 3b). Meanwhile, DTG peaks at 347 and 316 °C start to appear. And their intensities increased as the initial DPH concentrations increased. These latter DTG peaks might be attributed to decomposition of intercalated DPH under a monolayer and bilayer configuration (see discussions on simulation).

The continuous changes in weight loss on thermogravimetric (TG) analyses and increases in peak height on DTG analyses reflected systematic dehydration on the one hand, and slightly increased DPH thermal stability in the interlayer space of smectite on the other hand. The intercalation of DPH into the interlayer of smectite could also explain the extreme

stability of DPH in loam soil and to the overall formation of non-extractable soil-bound residues that was the major mechanism of DPH dissipation (Topp et al., 2012). The steady substitution of water molecules in the interlayer space of montmorillonite by drugs phenyl salicylate, methyl cinnamate, and ethyl cinnamate was observed in differential thermal and TG analyses (Del Hoyo et al., 1996). Similarly, dehydration of montmorillonite after intercalation of organic cations such as methylene blue and chlorpheniramine into the interlayer of montmorillonite was also noticed (Li et al., 2011b,c).

### 3.3. FTIR analyses

Although the samples were scanned from 450 to 4000  $\text{cm}^{-1}$ , vibrations in the range of 600–1800  $\text{cm}^{-1}$  were plotted in Fig. 4. The vibrations at 702 and 756  $\text{cm}^{-1}$  were assigned to C–H out-of-plane bending vibration of mono-substituted phenyl (Chapman, 1963; de Roos, 1967), while those at 714 and 756  $\text{cm}^{-1}$  were assigned to C–H out-of-plane deformation of mono-substituted phenyl (Nandgude et al., 2008). After DPH intercalation into smectite, the bands at 702 and 714  $\text{cm}^{-1}$  became into a single broad band at 706  $\text{cm}^{-1}$  (Fig. 5a). The non-resolved phenyl vibration might indicate the rigidity of the rings once intercalated into the interlayer of smectite.

The vibrations at 1380 and 1460  $\text{cm}^{-1}$  were attributed to symmetric and asymmetric bending vibrations of methyl groups (de Roos, 1967). The 1470  $\text{cm}^{-1}$  was attributed to C–N<sup>+</sup> vibration. The 1490  $\text{cm}^{-1}$  was due to the C–C

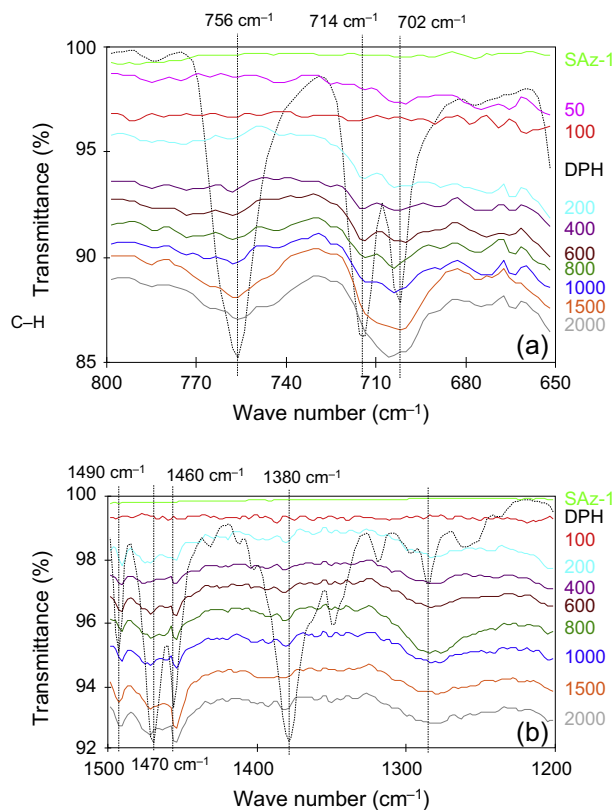


**Figure 5** FTIR analyses of SAz-1 in contact with DPH at different initial concentrations (mg/L) at 650–800  $\text{cm}^{-1}$  (a) and at 1200–1500  $\text{cm}^{-1}$  (b).

stretching vibration in the aromatic rings (de Roos, 1967) or to  $\nu(\text{C}=\text{C})$  (Ulu and Elmali, 2010). These bands were all present after DPH adsorption on the surface or intercalation into the interlayer of smectite (Fig. 5b). However, the  $1380\text{ cm}^{-1}$  band shifted slightly to higher wavenumbers while the  $1460\text{ cm}^{-1}$  band shifted to slightly lower wavenumbers. Meanwhile, the band at  $1470\text{ cm}^{-1}$  also shifted to slightly higher wavenumbers (Fig. 5b). These results may suggest the interactions between the negatively charged mineral surfaces and the  $\text{N}^+$  in the tertiary amine group.

### 3.4. Molecular simulation

DPH may take an extended or folded conformation when intercalating into swelling clays (Li et al., 2011a). Simulations were made to investigate which conformation was more favored. At the lower DPH adsorption level of about 0.2–0.3 CEC, the simulation using in a  $d_{001}$ -spacing of  $15.0\text{ \AA}$  resulted in a horizontal monolayer configuration of DPH in the interlayer of smectite with one of the diphenyl groups parallel to the surface (Fig. 6a and c). The nitrogen of DPH is located close to the center of the interlayer space (Fig. 6a and c). In contrast, at the DPH adsorption level of 0.6–0.7 CEC, the simulation using in a  $d_{001}$ -spacing of  $17.0\text{ \AA}$  revealed a bilayer conformation of the DPH molecules and close interactions between the two DPH molecules in the interlayer of SAz-1 (Fig. 6b and d). Meanwhile, the N atoms were closer to the mineral surfaces (Fig. 6b and d). However, the difference between the two conformations did not play a significant role in DPH intercalation.

### 3.5. Discussion

The change in d-spacing after DPH intercalation into smectite indicated interlayer adsorption, thus, interaction (Fig. 2). Previous studies on stoichiometric release of exchangeable cations accompanying DPH adsorption suggested the uptake of DPH by smectite was due to cation exchange (Li et al., 2011a). The continuous decrease in weight loss as the amount of DPH intercalation in smectite increased (Fig. 3a) and the increase in decomposition temperature of DPH in the interlayer of smectite also supported the substitution of hydrated cations by DPH occurred in the interlayer of smectite (Fig. 3b). The restricted vibration of certain DPH bands after DPH adsorption on smectite further confirmed the interlayer uptake (Figs. 4 and 5). Finally, the molecular simulation also revealed different interlayer configurations of DPH under lower and higher adsorption levels (Fig. 6). The configuration of DPH molecules in the interlayer of smectite was dependent on the amounts of DPH intercalation. A monolayer was the stable interlayer configuration with one of the diphenyl groups paralleling to the surface of the minerals when the initial DPH uptake was low (Fig. 6a). Under high DPH adsorption, the DPH molecules took a bilayer configuration in the interlayer of smectite. Previous molecular orbital calculation showed that the nitrogen in the neutral DPH molecules form had a charge of  $-0.064$ , but it increased to  $+0.525$  when DPH was in its ionic form (Zayed and El-Habeeb, 2010). This increased charge may explain the enhanced interactions between  $\text{N}^+$  and the negatively charge mineral surfaces and the significant increase in DPH uptake by the smectite.

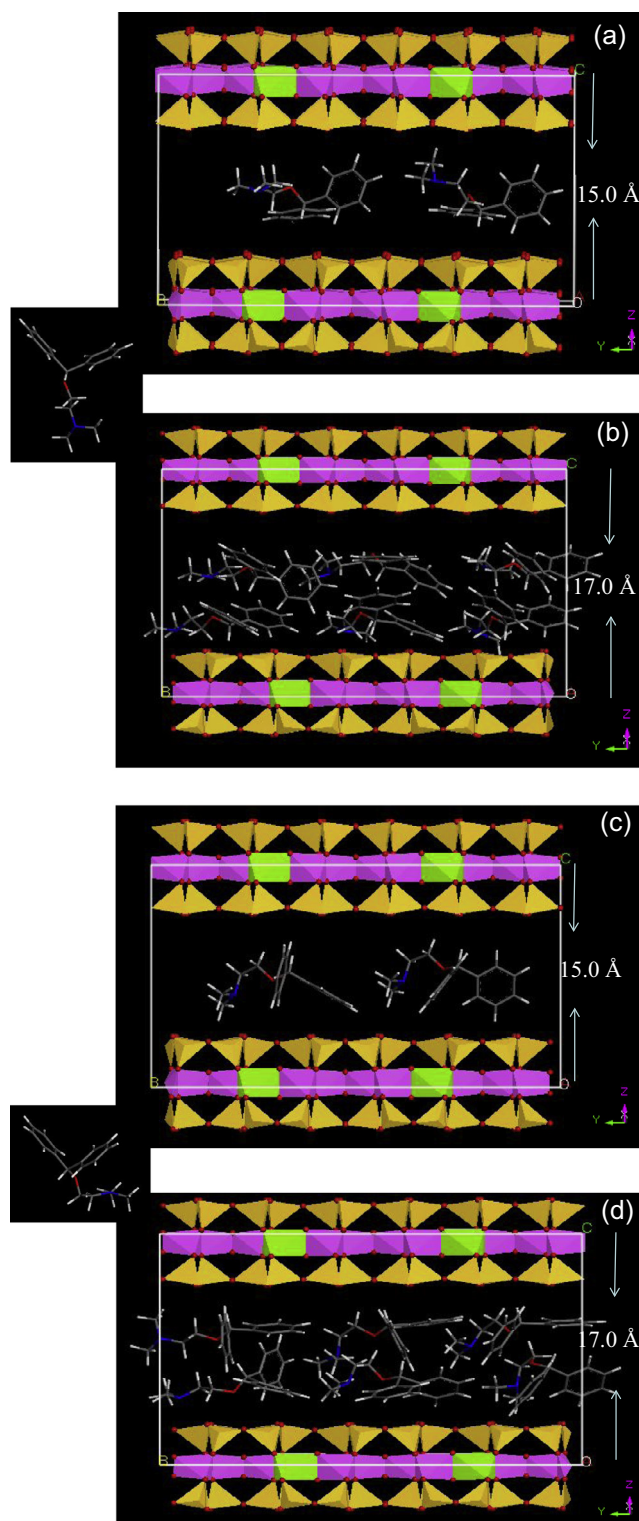


**Figure 6** Molecular dynamic simulation showing the configuration of DPH in the interlayer of SAz-1 under low (a, c) and high (b, d) amounts of DPH uptake using extended (a, b) and folded DPH conformation (c, d).

This study showed that the DPH, as one type of cationic drugs, had strong affinity for smectite minerals, which is an important soil component. The intercalation of cationic drugs into the interlayer of smectite associated with interlayer

dehydration would increase the thermal stability of intercalated drugs. This could be the ultimate cause for its prolonged environmental persistency and extended dissipation time in soil and water. Moreover, the intercalation of DPH into swelling clay minerals may shield itself from photocatalytic, chemical, or biological degradation, which might account for the widely detection of DPHs at the effluents from WWTPs even after wastewater treatment. On the other hand, the uptake of DPH was as high as 0.88 mmol/g or 0.25 g/g, far exceeding its uptake on AC (Guay et al., 1984). Thus, from the pharmacology point of view, the intercalation of DPH in smectite may suggest that smectite could be used as an alternative to AC to prevent drug overdose on the one hand, and the combined use of DPH and montmorillonite may generate antagonistic effect for the drug efficacy on the other hand. However, further studies on these issues are needed to confirm these speculations.

#### 4. Conclusions

The results of this research showed that the uptake of DPH by the smectite occurred on smectite surfaces as well as in the interlayer. Under a lower amount of DPH uptake at about 0.2–0.3 CEC of the minerals, the intercalated molecules took a horizontal monolayer configuration with one of the phenyl rings parallel to the mineral surface. This resulted in a  $d_{001}$  spacing expansion to 15 Å for the smectite. In contrast, at a higher amount of DPH uptake at 0.6–0.7 CEC of the mineral, the intercalated molecules arrange themselves into bilayer configuration regardless of whether the DPH took an extended or folded conformation. The  $d_{001}$  spacing of the smectite increased to 17 Å. The distance between the positively charged  $N^+$  in the tertiary amine group and the mineral surfaces was shorter, revealing that the electrostatic interaction between the positively charged tertiary amine and the negatively charged mineral surface was responsible for the DPH uptake. The intercalated DPH molecules were shielded by the minerals, resulting in an elevated decomposition temperature. The cation exchange of DPH for the hydrated  $Ca^{2+}$  resulted in significant dehydration of the minerals. The results may also suggest that antagonistic results would be anticipated if medicinal montmorillonite, which is used to treat diarrhea, and DPH, which is used to treat allergy, was taken simultaneously.

#### References

Agresti, C., Tu, Z.G., Ng, C., Yang, Y.S., Liang, J.F., 2008. *Eur. J. Pharm. Biopharm.* 70, 226–233.  
 Akkaramongkolporn, P., Wongsermsin, K., Opanasopit, P., Ngawhirunpat, T., 2010. *AAPS PharmSciTech* 11, 1104–1114.  
 Bartelt-Hunt, S.L., Snow, D.D., Damon, T., Shockley, J., Hoagland, K., 2009. *Environ. Pollut.* 157, 786–791.

Borden, D., Giese, R.F., 2001. *Clays Clay Miner.* 49, 444–445.  
 Breen, C., Madejová, J., Komadel, P., 1995. *J. Mater. Chem.* 5, 469–474.  
 Chapman, A.C., 1963. *Faraday Soc.* 59, 806–812.  
 Chipera, S.J., Bish, D.L., 2001. *Clays Clay Miner.* 49, 398–409.  
 de Roos, A.M., 1967. *Pharm. Weekblad.* 102, 1071–1077.  
 Del Hoyo, C., Rives, V., Vicente, M.A., 1996. *Thermochim. Acta* 286, 89–103.  
 Dogan, A.U., Dogan, M., Onal, M., Sarikaya, Y., Aburub, A., Wurster, D.E., 2006. *Clays Clay Miner.* 54, 62–66.  
 El-Shafey, El-S., Al-Lawati, H.A.J., Al-Hussaini, A.Y., 2014. *Chem. Ecol.* 30, 765–783.  
 Goolsby, E.W., Mason, C.M., Wojcik, J.T., Jordan, A.M., Black, M.C., 2013. *Environ. Toxicol. Chem.* 32, 2866–2869.  
 Guay, D.R., Meatherall, R.C., Macaulay, P.R., Yeung, C., 1984. *Int. J. Clin. Pharm. Ther. Toxicol.* 22, 395–400.  
 Guggenheim, S., Van Groos, A.F.K., 2001. *Clays Clay Miner.* 49, 433–443.  
 Kinney, C.A., Furlong, E.T., Zaugg, S.D., Burkhardt, M.R., Werner, S.L., Cahill, J.D., Jorgensen, G.R., 2006. *Environ. Sci. Technol.* 40, 7207–7215.  
 Li, Z., Chang, P.-H., Jiang, W.-T., Jean, J.-S., Hong, H., Liao, L., 2011a. *J. Colloid Interface Sci.* 360, 227–232.  
 Li, Z., Chang, P.-H., Jiang, W.-T., Jean, J.-S., Hong, H., 2011b. *Chem. Eng. J.* 168, 1193–1200.  
 Li, Z., Chang, P.-H., Jiang, W.-T., Jean, J.-S., Hong, H., 2011c. *Colloids Surf. A* 385, 213–218.  
 Li, X., Zheng, W., Kelly, W.R., 2013. *Sci. Total Environ.* 445, 22–28.  
 Mermut, A.R., Lagaly, G., 2001. *Clays Clay Miner.* 49, 393–397.  
 Mizuuchi, H., Katsura, T., Saito, H., Hashimoto, Y., Inui, K., 1999. *J. Pharm. Exp. Ther.* 290, 388–392.  
 Nandgude, T.D., Bhise, K.S., Gupta, V.B., 2008. *Indian J. Pharm. Sci.* 70, 482–486.  
 Nilsen, E., Furlong, E.T., Rosenbauer, R., 2014. *J. Am. Water Res. Assoc.* 50, 291–301.  
 Pastrana-Martínez, L.M., Morales-Torres, S., Likodimos, V., Figueiredo, J.L., Faria, J.L., Falaras, P., Silva, A.M., 2012. *Appl. Catal. B* 123, 241–256.  
 Scharman, E.J., Erdman, A.R., Wax, P.M., Chyka, P.M., Caravati, E.M., Nelson, L.S., Manoguerra, A.S., Christianson, G., Olson, K.R., Woolf, A.D., Keyes, D.C., Booze, L.L., Troutman, W.G., 2006. *Toxicology* 44, 205–223.  
 Tipparat, P., Lapanantnoppakhun, S., Jakmune, J., Grudpan, K., 2002. *J. Pharm. Biomed. Anal.* 30, 105–112.  
 Topp, E., Sumarah, M.W., Sabourin, L., 2012. *Sci. Total Environ.* 439, 136–140.  
 Ulu, S.T., Elmali, F.T., 2010. *Spectrochim. Acta Part A* 77, 324–329.  
 Walters, W., McClellan, K., Halden, R.U., 2010. *Water Res.* 44, 6011–6020.  
 Wu, C., Spongberg, A.L., Witter, J.D., Fang, M., Czajkowski, K.P., Ames, A., 2010a. *Arch. Environ. Contam. Toxicol.* 59, 343–351.  
 Wu, C., Spongberg, A.L., Witter, J.D., Fang, M., Czajkowski, K.P., 2010b. *Environ. Sci. Technol.* 44, 6157–6161.  
 Zayed, M.A., El-Habeeb, A.A., 2010. *Drug Test. Anal.* 2, 55–69.